



Original Article



TF-rs1049296 C>T Variant Modifies the Association between Hepatic Iron Stores and Liver Fibrosis in Metabolic Dysfunction-associated Steatotic Liver Disease

Sui-Dan Chen¹, Ka-Te Huang¹, Huai Zhang², Yang-Yang Li¹, Yi Jin¹, Hai-Yang Yuan³, Pei-Wu Zhu⁴, Jian-Min Li¹, Christopher D. Byrne⁵, Giovanni Targher^{6,7} and Ming-Hua Zheng^{3,8,9*}

¹Department of Pathology, the First Affiliated Hospital of Wenzhou Medical University, Wenzhou, Zhejiang, China; ²Department of Biostatistics and Medical Record, the First Affiliated Hospital of Wenzhou Medical University, Wenzhou, Zhejiang, China; ³MAFLD Research Center, Department of Hepatology, the First Affiliated Hospital of Wenzhou Medical University, Wenzhou, Zhejiang, China; ⁴Department of Clinical Laboratory, the First Affiliated Hospital of Wenzhou Medical University, Wenzhou, Zhejiang, China; ⁵Southampton National Institute for Health and Care Research, Biomedical Research Centre, University Hospital Southampton and University of Southampton, Southampton General Hospital, Southampton, UK; ⁶Department of Medicine, University of Verona, Verona, Italy; ⁷Metabolic Diseases Research Unit, IRCCS Sacro Cuore-Don Calabria Hospital, Negrar di Valpolicella, Italy; ⁸Institute of Hepatology, Wenzhou Medical University, Wenzhou, Zhejiang, China; ⁹Key Laboratory of Diagnosis and Treatment for The Development of Chronic Liver Disease in Zhejiang Province, Wenzhou, Zhejiang, China

Received: June 24, 2025 | Revised: November 08, 2025 | Accepted: November 20, 2025 | Published online: December 11, 2025

Abstract

Background and Aims: Hepatic iron deposition (HID) in the reticuloendothelial system (RES) is associated with histological severity in metabolic dysfunction-associated steatotic liver disease (MASLD). This study aimed to assess the interaction between the transferrin (TF)-rs1049296 C>T variant and HID patterns on the risk of significant liver fibrosis in MASLD. **Methods:** We analyzed 406 adults with liver biopsy-confirmed MASLD. HID was categorized as hepatocellular, RES, or mixed, based on Perl's iron staining. The association between iron-related genetic variants and significant liver fibrosis (fibrosis stage \geq F2) was analyzed, focusing on the interactions between single-nucleotide polymorphism genotypes and iron deposition patterns. Multivariable logistic regression analysis was used to adjust for potential confounders. **Results:** HID was detected in 271 (66.7%) patients, with hepatocellular, RES, and mixed patterns accounting for 11.1%, 18.0%, and 37.7%, respectively. A significant interaction was observed between HID and the TF-rs1049296 genotype ($P_{\text{interaction}} = 0.035$). In multivariable analysis, male sex, hypertension, severe lobular inflammation, and mixed hepatocellular/RES iron deposition were independent predictors of significant liver fibrosis. RES deposition markedly increased the risk of significant liver fibrosis (adjusted odds ratio: 6.65; 95% confidence interval: 1.84–23.97, $p < 0.05$), particularly

in men with isolated RES iron deposition (adjusted odds ratio: 5.26; 95% confidence interval: 1.21–22.81, $p < 0.05$). **Conclusions:** The TF-rs1049296 T allele interacts with RES iron deposition to identify a MASLD subpopulation at elevated risk of progressive liver disease, providing opportunities for refined risk stratification and personalized management.

Citation of this article: Chen SD, Huang KT, Zhang H, Li YY, Jin Y, Yuan HY, et al. TF-rs1049296 C>T Variant Modifies the Association between Hepatic Iron Stores and Liver Fibrosis in Metabolic Dysfunction-associated Steatotic Liver Disease. J Clin Transl Hepatol 2025. doi: 10.14218/JCTH.2025.00305.

Introduction

Metabolic dysfunction-associated steatotic liver disease (MASLD) is an emerging public health challenge, affecting nearly 30% of adults worldwide and increasing in parallel with the global rise in metabolic risk factors such as obesity, diabetes, and hypertension.^{1–3} It is projected to become a leading cause of end-stage hepatic disease in the coming decades.^{4,5} MASLD often begins with simple hepatic steatosis; however, inadequate control of metabolic risk factors can drive its progression to metabolic dysfunction-associated steatohepatitis (MASH), advanced fibrosis, cirrhosis, and hepatocellular carcinoma.^{6–10} The global prevalence of MASLD is projected to increase dramatically during the next decade, with the fastest growth expected in China, where liver-related mortality and late-stage liver disease mortality are expected to more than double.^{11,12}

MASLD is a complex and heterogeneous disease in which systemic iron homeostasis, normally regulated by the liver-

Keywords: Metabolic dysfunction-associated steatotic liver disease; MASLD; Nonalcoholic fatty liver disease; Iron deposition; Single-nucleotide polymorphism; Fibrosis.

***Correspondence to:** Ming-Hua Zheng, MAFLD Research Center, Department of Hepatology, the First Affiliated Hospital of Wenzhou Medical University, No. 2 Fuxue Lane, Wenzhou, Zhejiang 325000, China. ORCID: <https://orcid.org/0000-0003-4984-2631>. Tel: +86-577-55579611, Fax: +86-577-55578522, E-mail: zhengmh@wmu.edu.cn.

derived hormone hepcidin, is often disrupted.^{13,14} Hepcidin is a critical ferric homeostasis protein,¹⁵ and the regulatory mechanisms of hepcidin expression in MASLD patients have not been extensively investigated.¹⁶ Historically, hepatic iron was evaluated by histological staining of iron particles in liver biopsy specimens. Liver biopsy assessment remains central to studying the pathophysiology of iron-related parenchymal injury, inflammation, and fibrosis progression.¹⁷ Hyperferritinemia (HFE) is an independent long-term predictor of overall mortality in MASLD, but it is uncertain whether HFE is associated with greater significant fibrosis (SF) in the liver.^{18,19} The distribution of hepatic iron stores in liver diseases may follow one of three patterns: isolated hepatocellular iron deposition, isolated reticuloendothelial system (RES) deposition, or a mixed pattern involving both hepatocellular and RES deposition.^{18,20,21} Iron staining in RES is associated with histological features and progression to MASH and occurs only in hepatocytes or in a mixed pattern with milder liver disease.^{21,22} In Kupffer cells, the predominant non-parenchymal cell type in the liver, iron accumulation triggers the release of pro-inflammatory cytokines that activate hepatic stellate cells and contribute to liver fibrosis.²³ Therefore, the formation of hepatic fibrosis is influenced, to some extent, by hepatic iron deposition (HID), and excessive iron deposition may further promote the development of cirrhosis and hepatocellular carcinoma.²⁴ Thus, HID is considered a surrogate marker of hepatic fibrosis in both disease etiology and severity and is not merely a factor of fibrogenesis.²⁵

Previous studies have examined the relationship between HFE mutations and the severity of MASLD and concluded that HFE C282Y hybrid mutations were associated with advanced fibrosis in White individuals with MASH.²⁶ Genome-wide association studies conducted in Europe and Asia have identified many variations in transmembrane protease serine 6 (TMPRSS6) and transferrin (TF)-related genes that vary with iron status.²⁷ It has been reported that 36 single-nucleotide polymorphisms (SNPs) in TF, HFE, and TMPRSS6 genes were associated with iron status.²⁸ Critically, TF itself is a key component of the iron-sensing mechanism that regulates hepcidin. Diferric TF binds to TFR2 on hepatocytes to upregulate hepcidin via the BMP/SMAD pathway. TF variants (such as rs1049296) are postulated to disrupt this process by blunting the hepcidin response to iron, leading to inadequate suppression of iron absorption and potentially promoting HID.²⁹ In a small cohort of Italian patients with MASLD, variants of iron-related gene metabolism, particularly ceruloplasmin variants, were associated with higher serum ferritin levels, increased hepatic iron stores, and more severe liver disease.³⁰

Based on this background of evidence, this cross-sectional study aimed to examine whether TF-rs1049296 modulates the effect of HID distribution pattern on the risk of SF and whether there is an interaction between the HID distribution pattern and the TF-rs1049296 genetic variant, thus influencing the severity of liver disease, in a large cohort of Chinese individuals with biopsy-proven MASLD.

Methods

Patient population

This study involved a well-characterized epidemiological study of MASH (i.e., the "PERSONS" cohort study).³¹ We initially recruited 892 Han adult individuals with liver biopsy data (from December 2017 to February 2021). Among these individuals, 486 cases were excluded from the statistical analysis. The main reasons for exclusion were as follows: (1) fatty hepatic infiltration < 5% on liver histology; (2) body

mass index (BMI) < 23 kg/m²; (3) missing genotype data on the TF-rs1049296 genetic variant; and (4) missing serum ferritin data. Subjects with HFE genotypes at risk of iron overload (hemochromatosis), anemia, inflammation, and beta-thalassemia trait were excluded from the analysis. Due to these exclusions, a total of 406 individuals with biopsy-confirmed MASLD were included in the final analysis. Written informed consent was obtained from all participants. The study was approved by the Institutional Ethics Review Board of the First Affiliated Hospital of Wenzhou Medical University.

Diagnosis of MASLD

The diagnosis of MASLD was based on the presence of hepatic steatosis (≥5% on histology) in combination with one of the following three criteria: (1) overweight or obesity (BMI ≥ 23 kg/m² for the Asian population), (2) presence of type 2 diabetes, or (3) evidence of metabolic dysregulation.³² Given that our inclusion criteria required a BMI ≥ 23 kg/m², all participants in our final cohort fulfilled the MASLD diagnostic criteria. It is noteworthy that this patient population also aligns with the newly proposed definition of MASLD, as the core feature of metabolic dysfunction is central to both fatty liver disease nomenclatures.

Clinical and laboratory data

In all participants, we recorded demographics, anthropometric data, clinical parameters, and comorbidities. Biochemical variables were collected from all participants within 24 h of the liver biopsy examination. BMI was calculated as weight (kg) divided by the square of height (m). Insulin resistance was estimated by the homeostasis model assessment (HOMA-IR score).³³ Hypertension was defined as blood pressure ≥ 130/85 mmHg or antihypertensive treatment.³⁴ Diabetes was defined by a fasting plasma glucose level ≥ 7.0 mmol/L, hemoglobin A1c ≥ 6.5% (≥48 mmol/mol), or the use of any antihyperglycemic agents.³⁵

Quantification of HID patterns

Hepatic iron particle deposition refers to the accumulation of ferritin and hemosiderin in the hepatocytes and Kupffer cells. The staining principle is that the trivalent iron ion is separated from the protein by dilute hydrochloric acid in a solution of potassium ferricyanide, which reacts with the potassium ferricyanide to produce an insoluble blue compound, the ferricyanide Prussian blue of trivalent iron.³⁶

Significant iron deposition was defined as the presence of discernible hemosiderin granules. Hepatocellular iron was graded on a scale from 0 to 4, following the method established by Nelson *et al*.²¹ RES iron, representing iron within sinusoidal lining cells, was scored using a separate three-tiered scale: 0 (absent), 1 (mild), and 2 (more than mild). Based on these scores, the overall iron deposition pattern for each liver biopsy sample was categorized as predominantly hepatocellular iron, predominantly RES iron, or mixed hepatocellular and RES iron (indicating concurrent significant iron deposition in hepatocytes and reticuloendothelial cells).

To ensure diagnostic accuracy and consistency, all Prussian blue-stained slides were reviewed independently by two experienced liver pathologists who were blinded to the clinical and genetic data of participants. Any discrepant cases were re-examined jointly until a consensus was reached.

Histological liver assessment

Liver biopsies were performed using a 16-gauge needle under ultrasound guidance. Liver biopsy specimens were scored by an expert liver pathologist (Y-Y L), who was unaware of

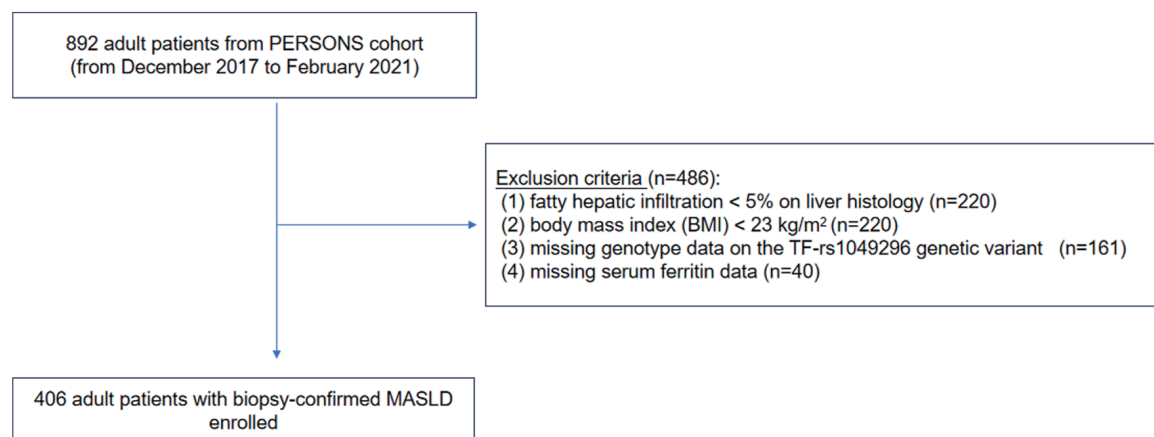


Fig. 1. Flowchart for the study. MASLD, metabolic dysfunction-associated steatotic liver disease; BMI, body mass index; TF, transferrin.

the participants' clinical details. Histologic scoring was based on the MASLD activity score.³⁷ SF was histologically defined by liver fibrosis \geq F2 stage.³⁸

Analysis of TF-rs1049296 polymorphism

Genotyping for the TF-rs1049296 variant was performed using the MassARRAY (Agena Biosciences, San Diego, CA, USA) or TaqMan assay (Bio-Rad, Hercules, CA, USA) platforms, according to the manufacturer's protocol. Each sample used approximately 20 ng of genomic DNA extracted from peripheral blood leukocytes for genotyping. Site-specific PCR and primer detections were designed by the corresponding detection design suite v3.1.

Statistical analysis

We used PLINK 1.9 for the QC of genomics data. We removed SNPs with (1) a MAF < 0.01 , (2) missing rate $> 5\%$, or (3) deviation from Hardy-Weinberg equilibrium (P -value $< 1 \times 10^{-6}$). We removed individuals with (1) a calling rate $< 5\%$, (2) inconsistent physiological and genetic sex, and (3) those who had pi-hat (i.e., second-degree relatives) > 0.2 with other individuals. We further removed individuals without any information about biopsy-proven or retained iron-related SNPs. Finally, the TF-rs1049296 variant was analyzed in the present analysis.

All data were analyzed with the R statistical package (The R Foundation; <http://www.r-project.org>; version 3.4.3) and Empower (R) (www.empowerstats.com; X&Y Solutions, Inc., Boston, MA, USA). Continuous variables were expressed as means \pm standard deviation or medians and interquartile ranges, depending on whether their distribution was normal or skewed, and the one-way ANOVA or the Kruskal-Wallis test was used for comparison. The categorical variables were expressed as proportions and compared using the chi-square test or Fisher's exact test as appropriate. Iron-related genes (i.e., TF, HFE, TIBC, TM6SF2, TMPRSS6, PNPLA3 genetic variants) were selected²⁸, and TF-rs1049296 was found to be associated with HID and liver fibrosis in genome-wide association studies. Factors associated with SF were assessed using univariable and multivariable logistic regression analyses. The association between different hepatic iron deposit locations and the presence of SF was tested by binary logistic regression analyses. These regression models were adjusted for potential confounders, such as age, BMI, HOMA-IR, and serum ferritin concentrations. Stratified and interaction analyses were also performed to examine the effect of TF-

rs1049296 polymorphism on the association between different hepatic iron deposit locations and SF. A P -value < 0.05 was considered statistically significant.

Results

Characteristics of hepatic iron staining patterns

As shown in Figure 1, 406 Chinese individuals with biopsy-confirmed MASLD were included in the final analysis. Significant differences in clinical and laboratory parameters among patients with different iron staining and those without hepatic iron staining are shown in Table 1. Stainable hepatic iron was found in 271 patients (66.7% of total), and three distinct patterns of hepatic iron staining were observed: hepatocellular [45/271 (16.6%)], RES [73/271 (26.9%)], or mixed pattern [153/271 (56.5%)]. Significant differences in staining patterns were found in women with increased BMI in the different HID groups, with the highest BMI values observed in the iron-located RES system group. According to hepatic iron staining patterns, there were also significant differences in total bilirubin, uric acid, HOMA-IR, triglycerides, high-sensitivity C-reactive protein, hemoglobin, serum iron, ferritin, and proportion of hypertension. In addition, there were also significant differences in the proportion of hepatocyte ballooning and fibrosis according to HID locations.

Effect of iron-related genes and HID location on liver fibrosis severity

Interaction tests for each SNP were based on independent biological hypotheses regarding their respective roles in iron metabolism. Therefore, each test was interpreted individually, and no correction for multiple comparisons was applied, consistent with the analysis of pre-specified candidate genes. According to the interaction analyses shown in Table 2, iron-related genes (SLC40A1 of chromosome 2, SPPRB of chromosome 3, HFE of chromosome 6, TIBC of chromosome 18, TM6SF2 of chromosome 19, TMPRSS6 and PNPLA3 of chromosome 22) and HID location did not show any significant interaction effect on the severity of hepatic fibrosis. Only TF-rs1049296 in chromosome 3 had a significant interaction with HID and hepatic fibrosis ($P_{\text{interaction}} = 0.035$).

Characteristics of participants stratified by TF-rs1049296 polymorphism genotypes

Table 3 summarizes the baseline characteristics of the study

Table 1. Comparison of clinical and laboratory parameters according to the hepatic iron deposit location

	No iron stains (n = 135)	HC iron only (n = 45)	RES iron only (n = 73)	Mixed HC/RES iron (n = 153)	P-value
Clinical parameters					
Female sex, n (%)	71 (52.6)	3 (6.7)	17 (23.3)	18 (11.8)	<0.001
Age, years	43.2 ± 12.8	38.4 ± 11.8	42.1 ± 14.0	42.8 ± 12.4	0.169
Body mass index, kg/m ²	27.5 ± 3.2	27.0 ± 2.9	28.9 ± 5.0	27.1 ± 3.2	0.003
Laboratory parameters					
Alanine aminotransferase, U/L	47.0 (26.5–82.5)	38.0 (25.0–82.0)	54.0 (35.0–101.0)	54.0 (32.0–87.0)	0.110
Aspartate aminotransferase, U/L	34.0 (23.5–58.0)	33.0 (21.0–48.0)	39.0 (27.0–71.0)	34.0 (25.0–52.0)	0.052
Gamma-glutamyltransferase, U/L	49.0 (27.5–84.5)	53.0 (35.0–105.0)	52.0 (36.0–107.0)	54.0 (36.0–75.0)	0.535
Total bilirubin, µmol/L	11.0 (8.0–14.5)	12.0 (9.0–14.0)	13.0 (9.0–16.0)	13.0 (10.0–18.0)	0.002
Uric acid, µmol/L	358.0 (305.0–433.0)	407.0 (364.0–474.0)	393.0 (330.0–477.0)	394.0 (335.0–477.0)	0.004
Fasting glucose, mmol/L	6.3 ± 1.8	5.6 ± 1.3	6.4 ± 3.0	6.0 ± 1.8	0.069
Fasting insulin, pmol/L	111.1 (69.7–171.6)	82.7 (62.3–142.9)	117.5 (87.6–165.4)	105.2 (68.6–152.1)	0.063
HOMA-IR score	4.0 (2.7–5.9)	2.7 (2.1–4.7)	4.5 (3.1–6.5)	3.8 (2.3–5.2)	0.012
Total cholesterol, mmol/L	5.1 ± 1.3	5.2 ± 1.2	5.4 ± 1.2	5.1 ± 1.2	0.301
Triglycerides, mmol/L	1.8 (1.2–2.6)	2.2 (1.6–2.9)	1.9 (1.5–2.9)	2.1 (1.4–3.2)	0.044
HDL-cholesterol, mmol/L	1.1 ± 0.4	1.0 ± 0.2	1.0 ± 0.2	1.0 ± 0.2	0.080
LDL-cholesterol, mmol/L	3.0 (2.4–3.6)	2.9 (2.5–3.6)	3.1 (2.6–3.7)	2.8 (2.3–3.4)	0.060
Platelet count, ×10 ⁹ /L	252.6 ± 59.0	264.6 ± 55.0	245.5 ± 54.7	239.5 ± 64.8	0.470
High-sensitivity C-reactive protein*, mg/L	1.6 (0.8–3.6)	1.8 (1.2–2.9)	1.2 (0.5–5.5)	1.1 (0.6–1.5)	0.034
Hemoglobin, g/L	140.9 ± 15.8	152.1 ± 11.4	149.2 ± 15.5	150.8 ± 12.8	<0.001
Iron, µmol/L	15.3 (11.7–18.7)	16.0 (13.3–18.2)	15.5 (13.6–20.2)	18.4 (13.9–23.3)	0.017
Transferrin concentrations**, %	23.5 (18.3–31.0)	30.50 (23.0–32.5)	27.50 (23.3–32.5)	33.00 (25.5–41.5)	0.637
Ferritin, mcg/L	142.5 (69.0–250.6)	281.2 (191.4–402.5)	291.3 (168.9–407.8)	419.3 (281.6–594.9)	<0.001
Comorbid diseases					
Type 2 diabetes, n (%)	60 (44.4)	10 (22.2)	30 (41.1)	58 (37.9)	0.065
Hypertension, n (%)	64 (47.4)	11 (24.4)	41 (56.2)	66 (43.1)	0.008
Dyslipidemia, n (%)	119 (88.8)	42 (93.3)	70 (95.9)	135 (89.4)	0.307
Histological liver features					
Steatosis, n (%)					0.374
Mild steatosis	59 (41.3)	23 (51.1)	27 (37.0)	73 (47.7)	
Severe steatosis	76 (56.3)	22 (48.9)	46 (63.0)	80 (52.3)	
Hepatocyte ballooning, n (%)					0.002
Mild ballooning	73 (54.1)	33 (73.3)	32 (43.8)	100 (65.4)	
Severe ballooning	62 (45.9)	15 (26.7)	41 (56.2)	53 (34.6)	
Lobular inflammation, n (%)					0.487
Mild inflammation	81 (60.0)	30 (66.7)	40 (54.8)	98 (64.1)	
Severe inflammation	54 (40.0)	15 (33.3)	33 (45.2)	55 (35.9)	
Fibrosis stage, n (%)					0.029
No-significant fibrosis	106 (78.5)	40 (88.9)	48 (65.8)	119 (77.8)	
Significant fibrosis	29 (21.5)	5 (11.1)	25 (34.2)	34 (22.2)	

Categorical variables are expressed as numbers (percentages), and continuous variables are presented as means ± SD for normally distributed variables or medians and interquartile ranges (IQR) for non-normally distributed variables. Differences in continuous variables among the groups were determined using one-way ANOVA and the Kruskal-Wallis test. *P*-value < 0.05 is bolded for statistical significance. *Data were available only in 325 patients. **Data were available only in 153 patients. HC, hepatocellular; RES, reticuloendothelial system; HOMA-IR, homeostasis model assessment of insulin resistance.

Table 2. Effects of iron-related genes and locations of hepatic iron deposition on the severity of liver fibrosis

Locus	Gene	Location of hepatic iron deposition			P-value (interaction)
		HC iron only	RES iron only	Mixed HC/RES iron	
CHR 2					
rs994227 T > C	SLC40A1	0.52 (0.19–1.47)	2.04 (1.06–3.96)	0.94 (0.52–1.71)	0.483
CHR 3					
rs1830084 A > T	TF	0.51 (0.11–2.46)	1.21 (0.46–3.18)	1.11 (0.56–2.64)	0.562
rs1799852 C > T	TF	0.46 (0.92–2.34)	1.63 (0.58–4.55)	0.96 (0.37–2.49)	0.995
rs2280673 A > C	TF	0.20 (0.24–1.66)	1.44 (0.51–4.04)	0.63 (0.25–1.59)	0.814
rs3811647 G > A	TF	0.56 (0.11–2.89)	2.74 (1.07–6.99)	1.08 (0.45–2.59)	0.625
rs1880669 T > C	TF	0.43 (0.05–3.92)	5.00 (1.62–15.44)	1.43 (0.49–4.16)	0.307
rs1358024 C > T	TF	0.64 (0.12–3.27)	3.42 (1.35–8.68)	1.48 (0.62–3.52)	0.432
rs1525892 G > A	TF	0.56 (0.11–2.89)	2.74 (1.07–6.99)	1.08 (0.45–2.59)	0.625
rs3811658 C > T	TF	0.55 (0.11–2.82)	2.82 (1.10–7.26)	1.10 (0.46–2.65)	0.757
rs8177248 C > T	TF	0.55 (0.11–2.82)	2.82 (1.10–7.26)	1.10 (0.46–2.65)	0.729
rs7638018 A > G	TF	0.56 (0.11–2.89)	2.60 (1.02–6.59)	1.08 (0.45–2.59)	0.591
rs1049296 C > G	TF	0.89(0.11–6.98)	6.83(1.78–26.14)	1.71(0.55–5.27)	0.035
CHR 6					
rs1799945 C > G	HFE	0.47 (0.17–1.31)	1.62 (0.85–3.07)	0.94 (0.53–1.67)	0.973
CHR 18					
rs9948708 G > A	TIBC	0.67 (0.17–2.64)	1.33 (0.48–3.70)	0.84 (0.35–2.00)	0.979
CHR 19					
rs58542926 C > T	TM6SF2	0.55 (0.20–1.56)	1.62 (0.81–3.26)	0.87 (0.46–1.62)	0.950
CHR 22					
rs855791 A > G	TMPRSS6	0.34 (0.04–2.93)	0.74 (0.21–2.66)	1.13 (0.38–3.37)	0.530
rs4820268 G > A	TMPRSS6	0.30 (0.03–2.68)	0.68 (0.21–2.26)	0.68 (0.22–2.11)	0.572
rs1421312 A > G	TMPRSS6	0.26 (0.03–2.19)	1.56 (0.55–4.49)	0.93 (0.35–2.48)	0.801
rs2111833 C > T	TMPRSS6	0.27 (0.03–2.24)	1.31 (0.50–3.46)	0.83 (0.32–2.12)	0.674
rs738409 C > G	PNPLA3	1.17 (0.19–7.07)	1.54 (0.31–7.69)	1.38 (0.36–5.31)	0.495

Data were presented as odds ratios and 95% confidence intervals and tested by univariable logistic regression analysis. *P*-value_(interaction) represents the interaction between iron-related genes and hepatic iron deposition distribution on the severity of liver fibrosis. The reference category is the "No iron stain" group. *P*-value < 0.05 is bolded for statistical significance. HC, hepatocellular; RES, reticuloendothelial system; CHR, chromosome; TF, transferrin; HFE, hyperferritinemia; TIBC, total iron-binding capacity; TM6SF2, transmembrane 6 superfamily 2; TMPRSS6, transmembrane protease serine 6; PNPLA3, patatin-like phospholipase domain-containing protein 3.

participants, stratified by the TF-rs1049296 polymorphism genotypes. The distribution of TF-rs1049296 genotypes was as follows: 204 (50.2%) had the CC genotype, and 202 (49.8%) had the (CT+TT) genotype. This genotype distribution did not deviate from the Hardy–Weinberg equilibrium. The distribution of main clinical variables, laboratory parameters, comorbid diseases, and histological liver features by TF-rs1049296 polymorphism genotypes is shown in Table 3.

Multivariable regression analysis of factors associated with SF

Multivariable logistic regression analysis was performed to identify independent factors associated with SF, as shown in Table 4. In univariable regression analysis, male sex, higher BMI, increased serum liver enzymes (alanine aminotransferase, aspartate aminotransferase), insulin resistance (HOMA-IR, fasting insulin), type 2 diabetes, and hypertension, as well as severe histological features (steatosis, ballooning, and inflammation), and the presence of RES iron deposition

were significantly associated with SF. However, in a multivariable regression model adjusted for potential confounding factors, only male sex (adjusted odds ratio (OR) 0.28, 95% confidence interval (CI) 0.13–0.60, *p* = 0.001), hypertension (adjusted OR 1.90, 95% CI 1.05–3.45, *p* = 0.035), and severe lobular inflammation (adjusted OR 8.40, 95% CI 4.29–16.44, *p* < 0.001) were independently associated with SF. Conversely, the TF-rs1049296 genotype was not independently associated with SF.

TF-rs1049296 variant influences the association between different HID localizations and SF

Multivariable logistic regression modeling was undertaken to better understand the association between the TF-rs1049296 variant and SF in patients with different HID localizations. As shown in Table 5, the rs1049296 T/T + C/T genotypes were associated with an increased risk of SF, with an OR of 6.65 (T/T + C/T vs. C/C, 95% CI 1.84–23.97, *p* < 0.05) for the dominant model after adjusting for age, BMI, hemoglobin,

Table 3. Characteristics of study participants, stratified by TF-rs1049296 polymorphism

	C/C (n = 204)	C/T +T/T (n = 202)	P-value
Clinical parameters			
Female sex, n (%)	59 (28.9)	50 (24.8)	0.343
Age, years	43.8 ± 13.2	40.9 ± 12.3	0.024
Body mass index, kg/m ²	27.4 ± 2.9	27.7 ± 4.2	0.822
Laboratory parameters			
Alanine aminotransferase, U/L	48.0 (27.0–83.0)	53.5 (30.0–94.0)	0.341
Aspartate aminotransferase, U/L	35.0 (25.0–57.0)	34.0 (24.0–56.0)	0.518
Gamma-glutamyl transferase, U/L	53.0 (31.0–84.2)	53.0 (35.0–86.8)	0.554
Total bilirubin, µmol/L	12.0 (9.0–16.0)	12.0 (9.0–16.0)	0.982
Uric acid, µmol/L	375.5 (313.8–446.0)	393.0 (332.0–474.0)	0.063
Fasting glucose, mmol/L	6.0 ± 1.8	6.2 ± 2.2	0.737
Fasting insulin, pmol/L	106.7 (69.2–148.2)	109.0 (73.1–161.0)	0.361
HOMA-IR score	3.8 (2.3–5.4)	3.9 (2.5–6.0)	0.241
Total cholesterol, mmol/L	5.1 ± 1.3	5.2 ± 1.2	0.451
Triglycerides, mmol/L	2.0 (1.3–2.8)	2.0 (1.5–3.0)	0.379
HDL-cholesterol, mmol/L	1.0 ± 0.3	1.0 ± 0.2	0.121
LDL-cholesterol, mmol/L	2.9 (2.3–3.6)	3.0 (2.4–3.6)	0.564
Platelet count, ×10 ⁹ /L	234.7 ± 58.0	253.6 ± 66.1	0.009
High-sensitivity C-reactive protein*, mg/L	1.2 (0.6–2.2)	1.3 (0.7–2.9)	0.147
Hemoglobin, g/L	146.7 ± 14.7	148.0 ± 15.1	0.307
Iron, µmol/L	16.70 (13.40–21.90)	17.0 (12.9–19.9)	0.323
Transferrin concentrations**, %	29.0 (22.5–38.5)	29.0 (22.0–34.8)	0.445
Ferritin, mcg/L	301.4 (151.1–440.0)	272.4 (148.2–440.5)	0.298
Comorbid diseases			
Type 2 diabetes, n (%)	83 (40.7)	75 (37.1)	0.462
Hypertension, n (%)	89 (43.6)	93 (46.0)	0.625
Dyslipidemia, n (%)	183 (90.1)	183 (91.5)	0.638
Histological liver features			
Steatosis, n (%)			0.757
Mild steatosis	93 (45.6)	89 (44.1)	
Severe steatosis	111 (54.4)	113 (55.9)	
Hepatocyte ballooning, n (%)			0.627
Mild ballooning	122 (59.8)	116 (57.4)	
Severe ballooning	82 (40.2)	86 (42.6)	
Lobular inflammation, n (%)			0.556
Mild inflammation	128 (62.7)	121 (59.9)	
Severe inflammation	76 (37.3)	81 (40.1)	
Fibrosis stage, n (%)			0.176
No-significant fibrosis	163 (79.9)	150 (74.3)	
Significant fibrosis	41 (20.1)	52 (25.7)	

Categorical variables are expressed as numbers (percentages), and continuous variables are presented as means ± SD for normally distributed variables or medians and interquartile ranges (IQR) for non-normally distributed variables. Differences in continuous variables among the patient groups were determined by one-way ANOVA and the Kruskal-Wallis test. *Data were available only in 325 patients. **Data were available only in 153 patients. TF, transferrin; HOMA-IR, homeostasis model assessment of insulin resistance.

Table 4. Univariable and multivariable logistic regression analysis of factors associated with fibrosis stage

	Univariable analysis	P-value	Multivariable analysis	P-value
Clinical parameters				
Sex		0.002		0.001
Female	1.0		1.0	
Male	0.45 (0.28, 0.74)		0.28 (0.13, 0.60)	
Age, years	1.01 (1.00, 1.03)	0.149		
Body mass index, kg/m ²	1.12 (1.05, 1.19)	<0.001		
Laboratory parameters				
Alanine aminotransferase, U/L	1.01 (1.00, 1.01)	<0.001		
Aspartate aminotransferase, U/L	1.02 (1.01, 1.02)	<0.001		
Gamma-glutamyl transferase, U/L	1.00 (0.99, 1.01)	0.072		
Total bilirubin, µmol/L	1.15 (0.95, 1.38)	0.492		
Uric acid, µmol/L	1.00 (0.99, 1.00)	0.890		
Fasting glucose, mmol/L	1.00 (1.00, 1.01)	0.060		
Fasting insulin, pmol/L	1.16 (1.04, 1.29)	0.006		
HOMA-IR score	1.03 (1.00, 1.05)	0.039		
Total cholesterol, mmol/L	1.15 (0.95, 1.38)	0.155		
Triglycerides, mmol/L	0.96 (0.84, 1.10)	0.547		
HDL-cholesterol, mmol/L	1.73 (0.80, 3.75)	0.165		
LDL-cholesterol, mmol/L	1.08 (0.84, 1.38)	0.558		
Platelet count, ×10 ⁹ /L	0.99 (0.99, 1.00)	0.516		
High-sensitivity C-reactive protein*, mg/L	1.03 (0.97, 1.08)	0.332		
Hemoglobin, g/L	1.00 (0.98, 1.01)	0.566		
Iron, µmol/L	1.03 (0.97, 1.09)	0.361		
Transferrin concentrations**	1.01 (0.98, 1.05)	0.447		
Ferritin, mcg/L	1.00 (0.99, 1.00)	0.172		
Comorbid diseases				
Type 2 diabetes		0.005		
	1.0			
	1.97 (1.23, 3.14)			
Hypertension		<0.001		0.035
	1.0		1.0	
	2.25 (1.40, 3.60)		1.90 (1.05, 3.45)	
Dyslipidemia		0.524		
	1.0			
	0.78 (0.36, 1.68)			
Histological liver features				
Steatosis		<0.001		
Mild steatosis	1.0			
Severe steatosis	3.14 (1.87, 5.29)			
Hepatocyte ballooning		<0.001		
Mild ballooning	1.0			
Severe ballooning	3.25 (2.01, 5.26)			

(continued)

Table 4. (continued)

	Univariable analysis	P-value	Multivariable analysis	P-value
Lobular inflammation		<0.001		<0.001
Mild inflammation	1.0		1.0	
Severe inflammation	9.95 (5.72, 17.32)		8.40 (4.29, 16.44)	
Distribution of iron deposition		0.035		
No iron stains	1.0		1.0	
HC iron only	0.46 (0.17, 1.26)	0.131		
RES iron only	1.90 (1.01, 3.59)	0.047	2.31 (0.98, 5.43)	0.054
Mixed HC/RES iron	1.04 (0.60, 1.83)	0.879	2.53 (1.18, 5.43)	0.017
TF rs1049296				
Dominant model		0.177		
C/C	1.0			
T/T+C/T	1.38 (0.87, 2.20)			

Data are expressed as odds ratios and 95% confidence intervals as tested by univariable and multivariable logistic regression analyses. Variables significant in univariable analysis ($p < 0.05$) were included in the multivariate analyses. Ref. = reference category. P -value < 0.05 is bolded for statistical significance. *Data were available only in 325 patients. **Data were available only in 153 patients. TF, transferrin; HOMA-IR, homeostasis model assessment of insulin resistance; HC, hepatocellular; RES, reticuloendothelial system.

HOMA-IR, and serum ferritin concentrations. This association was especially evident in men with isolated RES iron, where the T allele conferred an adjusted OR of 5.26 (95% CI 1.21–22.81, $p < 0.05$) for SF. Conversely, in this model, the TF-rs1049296 variant was not associated with SF in the context of other iron deposition patterns (no iron, hepatocellular iron only, or mixed hepatocellular/RES iron), highlighting the specificity of the gene–environment interaction between the T allele and RES iron in driving liver fibrosis progression.

Discussion

In this cross-sectional study of Chinese individuals with biopsy-proven MASLD, we showed a novel gene–environment

interaction driving liver fibrosis progression, i.e., the synergy between the TF-rs1049296 T allele and RES iron deposition. To our knowledge, this specific gene–environment interaction has not been previously reported and provides a possible mechanistic link between genetic predisposition in systemic iron transport and localized iron-driven inflammation in hepatic macrophages.

Although it is known that tissue iron excess can damage the liver by inducing oxidative stress and lipid peroxidation,^{21,39,40} the effects of hepatic iron accumulation on hepatic fibrogenesis are not fully understood. In recent years, it has been appreciated that the genetic background plays an important role in the development and progression of MASLD. Patients with MASLD tend to accumulate iron in the

Table 5. Association between TF-rs1049296 genotype and liver fibrosis, stratified by sex and hepatic iron deposition

Stratification	Iron Deposition	Genotype	Unadjusted	Adjusted
Total	No iron stain	T/T+C/T	0.75 (0.33, 1.72)	0.95 (0.37, 2.48)
	HC iron only	T/T+C/T	0.67 (0.10, 4.43)	1.39 (0.10, 19.77)
	RES iron only	T/T+C/T	5.14 (1.78, 14.84)*	6.65 (1.84, 23.97)*
	Mixed HC/RES	T/T+C/T	1.29 (0.60, 2.77)	1.16 (0.50, 2.70)
Female	No iron stain	T/T+C/T	1.32 (0.47, 3.72)	2.74 (0.69, 10.80)
	HC iron only	T/T+C/T	/	/
	RES iron only	T/T+C/T	/	/
	Mixed HC/RES	T/T+C/T	0.60 (0.09, 3.99)	1.59 (0.12, 20.56)
Male	No iron stain	T/T+C/T	0.33 (0.08, 1.47)	0.26 (0.05, 1.36)
	HC iron only	T/T+C/T	0.33 (0.03, 3.50)	0.86 (0.03, 25.98)
	RES iron only	T/T+C/T	4.29 (1.25, 14.68)*	5.26 (1.21, 22.81)*
	Mixed HC/RES	T/T+C/T	1.63 (0.68, 3.91)	1.47 (0.56, 3.85)

All analyses used the C/C genotype as the reference group. Data are expressed as odds ratios and 95% confidence intervals as tested by univariable and multivariable logistic regression analyses. /: denotes that the calculation was precluded by a subgroup sample size too small for reliable estimations. *indicates P -value < 0.05 . Adjusted regression model: age, body mass index, hemoglobin, HOMA-IR, and serum ferritin concentrations. HC, hepatocellular; RES, reticuloendothelial system; TF, transferrin; HOMA-IR, homeostasis model assessment of insulin resistance.

hepatocytes and macrophages, possibly due to various factors (genetics, hepatic inflammation, and leakage of dead hepatocytes with subsequent phagocytosis by hepatic macrophages).⁴¹

Liver fibrosis has been identified as a meaningful prognostic factor in individuals with MASLD.⁴² Previously, we have reported the presence of hepatic iron stores in the RES in over 10% of patients with MASLD,²¹ which disrupts the balance between M1/M2 macrophage polarization, thus leading to macrophage-driven hepatic inflammation and fibrosis in MASLD.⁴³

The TF-rs1049296 variant, also known as Pro570Ser, is known to be the basis for the C1/C2 subtypes of the TF gene. The rs1049296 (C) allele encodes the C1 subtype, while the rarer rs1049296 (T) allele encodes the C2 subtype. We propose a mechanistic link whereby the T allele (C2 subtype), associated with systemic iron overload and increased iron flux to the liver, exacerbates iron accumulation within RES macrophages (Kupffer cells). In the inflammatory milieu of MASLD, the iron overload increases oxidative stress through the Fenton reaction, driving Kupffer cells toward a profibrotic phenotype and the release of mediators (e.g., transforming growth factor- β) that directly promote hepatic fibrogenesis.⁴⁴ This gene-environment interaction postulates that the TF-rs1049296 T allele increases the iron burden presented to the liver, while RES iron deposition reflects an inflammatory microenvironment that primes macrophages for iron-driven activation. The convergence of these factors creates a synergistic effect, profoundly exacerbating iron-mediated oxidative stress and profibrotic signaling. The plausibility of this model is supported by functional evidence demonstrating that the TF receptor 2 variant synergizes with other iron-loading mutations, amplifying pathological iron overload and associated end-organ damage.⁴⁵

The major strengths of our study are as follows: first, it is the first study to examine a cohort of Asian individuals with hepatic iron in MASLD; second, liver biopsy specimens were rigorously analyzed using widely validated criteria, with assessments reviewed by a panel of expert liver pathologists and final confirmation by a single senior pathologist, ensuring both accuracy and consistency in histological evaluation.

This study also has several limitations that should be considered when interpreting the results. First, the cross-sectional design of our study precludes the establishment of causal relationships between the observed genetic factors, iron deposition, and severity of liver fibrosis. Second, the lack of detailed dietary iron intake data limits our ability to delineate the contribution of dietary sources versus inherent metabolic dysregulation to hepatic iron overload. Finally, our study cohort consisted of individuals of Asian descent; therefore, the generalizability of our findings to other ethnic populations requires further validation, as genetic backgrounds and environmental exposures can differ significantly.

Conclusions

In this large cross-sectional study, we identified a novel iron-related genetic susceptibility gene (i.e., the TF-rs1049296 variant) for MASLD. The T allele is significantly associated with a higher risk of SF in the RES pattern, and the interaction between genotype and different HID locations may increase the risk of SF. Further studies are needed to confirm these findings in other independent cohorts of patients with MASLD from different countries.

Funding

This work was funded by grants from the National Natural

Science Foundation of China (82070588), High-Level Creative Talents from the Department of Public Health in Zhejiang Province (S2032102600032), and the Project of New Century 551 Talent Nurturing in Wenzhou. GT is supported in part by grants from the School of Medicine, University of Verona, Verona, Italy. CDB is supported in part by the Southampton NIHR Biomedical Research Centre (NIHR203319), UK. CDB has received research grant support from Echosens, the manufacturer of the Fibroscan device used to assess liver fat and fibrosis in chronic liver diseases.

Conflict of interest

MHZ has been an Associate Editor of *Journal of Clinical and Translational Hepatology* since 2013, GT has been an Editorial Board Member of *Journal of Clinical and Translational Hepatology* since 2018. The other authors have no conflict of interests related to this publication.

Author contributions

Conceptualization (SDC, MHZ), data curation (SDC, KTH, HZ, YYL, YJ, HYY, PWZ), methodology (SDC), writing-original draft (SDC), investigation (KTH, HZ, YJ, HYY, PWZ, JML, GT, CDB, MHZ), clinical data management & entry (KTH), pathology sectioning & reading (YYL), writing-review & editing (JML, GT, CDB, MHZ), and project administration (MHZ). All authors contributed to the manuscript for important intellectual content and approved the final submission of the manuscript.

Ethical statement

The study was conducted in accordance with the Helsinki Declaration as revised in 2024 and approved by the Institutional Ethics Review Board of the First Affiliated Hospital of Wenzhou Medical University (No. KY2016-246). Written informed consent was obtained from all participants.

Data sharing statement

The data supporting the findings of this study are available from the corresponding author (zhengmh@wmu.edu.cn) upon reasonable request. Access to specific data may require approval from the corresponding author and compliance with relevant ethical guidelines.

References

- [1] Feng G, Valenti L, Wong VW, Fouad YM, Yilmaz Y, Kim W, *et al*. Recompensation in cirrhosis: unravelling the evolving natural history of nonalcoholic fatty liver disease. *Nat Rev Gastroenterol Hepatol* 2024;21(1):46–56. doi:10.1038/s41575-023-00846-4, PMID:37798441.
- [2] Byrne CD, Targher G. NAFLD: a multisystem disease. *J Hepatol* 2015;62(1 Suppl):S47–S64. doi:10.1016/j.jhep.2014.12.012, PMID:25920090.
- [3] Zhou XD, Chen QF, Targher G, Byrne CD, Mantzoros CS, Zhang H, *et al*. Global burden of disease attributable to metabolic risk factors in adolescents and young adults aged 15–39, 1990–2021. *Clin Nutr* 2024;43(12):391–404. doi:10.1016/j.clnu.2024.11.016, PMID:39579593.
- [4] Younossi Z, Anstee QM, Marietti M, Hardy T, Henry L, Eslam M, *et al*. Global burden of NAFLD and NASH: trends, predictions, risk factors and prevention. *Nat Rev Gastroenterol Hepatol* 2018;15(1):11–20. doi:10.1038/nrgastro.2017.109, PMID:28930295.
- [5] Zhang H, Zhou XD, Shapiro MD, Lip GYH, Tilg H, Valenti L, *et al*. Global burden of metabolic diseases, 1990–2021. *Metabolism* 2024;160:155999. doi:10.1016/j.metabol.2024.155999, PMID:39151887.
- [6] Rinella ME, Lazarus JV, Ratzliff V, Francque SM, Sanyal AJ, Kanwal F, *et al*. A multisociety Delphi consensus statement on new fatty liver disease nomenclature. *J Hepatol* 2023;79(6):1542–1556. doi:10.1016/j.jhep.2023.06.003, PMID:37364790.
- [7] Zhou XD, Chen QF, Kim SU, Cheuk-Fung Yip T, Petta S, Nakajima A, *et al*. Long-Term Glycemic Control and the Risk of Liver Stiffness Progression and Liver-Related Events in MASLD. *Clin Gastroenterol Hepatol* 2025.

- doi:10.1016/j.cgh.2025.10.003, PMID:41076043.
- [8] Fan JG, Xu XY, Yang RX, Nan YM, Wei L, Jia JD, *et al*. Guideline for the Prevention and Treatment of Metabolic Dysfunction-associated Fatty Liver Disease (Version 2024). *J Clin Transl Hepatol* 2024;12(11):955–974. doi:10.14218/JCTH.2024.00311, PMID:39544247.
 - [9] Wang TY, George J, Zheng MH. Metabolic (dysfunction) associated fatty liver disease: more evidence and a bright future. *Hepatobiliary Surg Nutr* 2021;10(6):849–852. doi:10.21037/hbsn-21-352, PMID:35004952.
 - [10] Zhou XD, Lian LY, Chen QF, Kim SU, Cheuk-Fung Yip T, Petta S, *et al*. Effect of hypertension on long-term adverse clinical outcomes and liver fibrosis progression in MASLD. *J Hepatol* 2025. doi:10.1016/j.jhep.2025.08.017, PMID:40854336.
 - [11] Estes C, Anstee QM, Arias-Loste MT, Bantel H, Bellentani S, Caballeria J, *et al*. Modeling NAFLD disease burden in China, France, Germany, Italy, Japan, Spain, United Kingdom, and United States for the period 2016–2030. *J Hepatol* 2018;69(4):896–904. doi:10.1016/j.jhep.2018.05.036, PMID:29886156.
 - [12] Li X, Zhou XD, Wu J, Zhao Z, Xie F, Li Y, *et al*. Pediatric MASLD in China: epidemiology, screening, diagnosis, and management. *Lancet Reg Health West Pac* 2025;64:101717. doi:10.1016/j.lanwpc.2025.101717, PMID:41158823.
 - [13] Younossi ZM. Non-alcoholic fatty liver disease - A global public health perspective. *J Hepatol* 2019;70(3):531–544. doi:10.1016/j.jhep.2018.10.033, PMID:30414863.
 - [14] Pigeon C, Ilyin G, Courselaud B, Leroyer P, Turlin B, Brissot P, *et al*. A new mouse liver-specific gene, encoding a protein homologous to human antimicrobial peptide hepcidin, is overexpressed during iron overload. *J Biol Chem* 2001;276(11):7811–7819. doi:10.1074/jbc.M008923200, PMID:11113132.
 - [15] Nemeth E, Tuttle MS, Powelson J, Vaughn MB, Donovan A, Ward DM, *et al*. Hepcidin regulates cellular iron efflux by binding to ferroportin and inducing its internalization. *Science* 2004;306(5704):2090–2093. doi:10.1126/science.1104742, PMID:15514116.
 - [16] Barisani D, Pelucchi S, Mariani R, Galimberti S, Trombini P, Fumagalli D, *et al*. Hepcidin and iron-related gene expression in subjects with Dysmetabolic Hepatic Iron Overload. *J Hepatol* 2008;49(1):123–133. doi:10.1016/j.jhep.2008.03.011, PMID:18462824.
 - [17] Bridle KR, Crawford DH, Fletcher LM, Smith JL, Powell LW, Ramm GA. Evidence for a sub-morphological inflammatory process in the liver in haemochromatosis. *J Hepatol* 2003;38(4):426–433. doi:10.1016/s0168-8278(02)00444-0, PMID:12663233.
 - [18] Buzzetti E, Petta S, Manuguerra R, Luong TV, Cabibi D, Corradini E, *et al*. Evaluating the association of serum ferritin and hepatic iron with disease severity in non-alcoholic fatty liver disease. *Liver Int* 2019;39(7):1325–1334. doi:10.1111/liv.14096, PMID:30851216.
 - [19] Chitturi S, Weltman M, Farrell GC, McDonald D, Kench J, Liddle C, *et al*. HFE mutations, hepatic iron, and fibrosis: ethnic-specific association of NASH with C282Y but not with fibrotic severity. *Hepatology* 2002;36(1):142–149. doi:10.1053/jhep.2002.33892, PMID:12085358.
 - [20] Brunt EM. Pathology of hepatic iron overload. *Semin Liver Dis* 2005;25(4):392–401. doi:10.1055/s-2005-923311, PMID:16315133.
 - [21] Nelson JE, Wilson L, Brunt EM, Yeh MM, Kleiner DE, Unalp-Arida A, *et al*. Relationship between the pattern of hepatic iron deposition and histological severity in nonalcoholic fatty liver disease. *Hepatology* 2011;53(2):448–457. doi:10.1002/hep.24038, PMID:21274866.
 - [22] Maliken BD, Nelson JE, Klintworth HM, Beauchamp M, Yeh MM, Kowdley KV. Hepatic reticuloendothelial system cell iron deposition is associated with increased apoptosis in nonalcoholic fatty liver disease. *Hepatology* 2013;57(5):1806–1813. doi:10.1002/hep.26238, PMID:23325576.
 - [23] Mehta KJ, Farnaud SJ, Sharp PA. Iron and liver fibrosis: Mechanistic and clinical aspects. *World J Gastroenterol* 2019;25(5):521–538. doi:10.3748/wjg.v25.i5.521, PMID:30774269.
 - [24] Xu Q, Xia W, Zhou L, Zou Z, Li Q, Deng L, *et al*. Determination of Hepatic Iron Deposition in Drug-Induced Liver Fibrosis in Rats by Confocal Micro-XRF Spectrometry. *ACS Omega* 2022;7(4):3738–3745. doi:10.1021/acsomega.1c06476, PMID:35128282.
 - [25] Guyader D, Thirouard AS, Erdtmann L, Rakba N, Jacquelinet S, Danielou H, *et al*. Liver iron is a surrogate marker of severe fibrosis in chronic hepatitis C. *J Hepatol* 2007;46(4):587–595. doi:10.1016/j.jhep.2006.09.021, PMID:17156889.
 - [26] Nelson JE, Bhattacharya R, Lindor KD, Chalasani N, Raaka S, Heathcote EJ, *et al*. HFE C282Y mutations are associated with advanced hepatic fibrosis in Caucasians with nonalcoholic steatohepatitis. *Hepatology* 2007;46(3):723–729. doi:10.1002/hep.21742, PMID:17680648.
 - [27] Jallow MW, Campino S, Prentice AM, Cerami C. Association of common TM-PRSS6 and TF gene variants with hepcidin and iron status in healthy rural Gambians. *Sci Rep* 2021;11(1):8075. doi:10.1038/s41598-021-87565-5, PMID:33850216.
 - [28] McLaren CE, McLachlan S, Garner CP, Vulpe CD, Gordeuk VR, Eckfeldt JH, *et al*. Associations between single nucleotide polymorphisms in iron-related genes and iron status in multiethnic populations. *PLoS One* 2012;7(6):e38339. doi:10.1371/journal.pone.0038339, PMID:22761678.
 - [29] Camaschella C, Nai A, Silvestri L. Iron metabolism and iron disorders revisited in the hepcidin era. *Haematologica* 2020;105(2):260–272. doi:10.3324/haematol.2019.232124, PMID:31949017.
 - [30] Corradini E, Buzzetti E, Dongiovanni P, Scarlini S, Caleffi A, Pelusi S, *et al*. Ceruloplasmin gene variants are associated with hyperferritinemia and increased liver iron in patients with NAFLD. *J Hepatol* 2021;75(3):506–513. doi:10.1016/j.jhep.2021.03.014, PMID:33774058.
 - [31] Li G, Tang LJ, Zhu PW, Huang OY, Rios RS, Zheng KI, *et al*. PNPLA3 rs738409 C>G Variant Influences the Association Between Visceral Fat and Significant Fibrosis in Biopsy-proven Nonalcoholic Fatty Liver Disease. *J Clin Transl Hepatol* 2022;10(3):439–448. doi:10.14218/JCTH.2021.00286, PMID:35836754.
 - [32] Eslam M, Newsome PN, Sarin SK, Anstee QM, Targher G, Romero-Gomez M, *et al*. A new definition for metabolic dysfunction-associated fatty liver disease: An international expert consensus statement. *J Hepatol* 2020;73(1):202–209. doi:10.1016/j.jhep.2020.03.039, PMID:32278004.
 - [33] Matthews DR, Hosker JP, Rudenski AS, Naylor BA, Treacher DF, Turner RC. Homeostasis model assessment: insulin resistance and beta-cell function from fasting plasma glucose and insulin concentrations in man. *Diabetologia* 1985;28(7):412–419. doi:10.1007/BF00280883, PMID:3899825.
 - [34] Alberti KG, Zimmet P, Shaw J. Metabolic syndrome—a new world-wide definition. A Consensus Statement from the International Diabetes Federation. *Diabet Med* 2006;23(5):469–480. doi:10.1111/j.1464-5491.2006.01858.x, PMID:16681555.
 - [35] Sabanayagam C, Khoo EY, Lye WK, Ikram MK, Lamoureux EL, Cheng CY, *et al*. Diagnosis of diabetes mellitus using HbA1c in Asians: relationship between HbA1c and retinopathy in a multiethnic Asian population. *J Clin Endocrinol Metab* 2015;100(2):689–696. doi:10.1210/jc.2014-2498, PMID:25375980.
 - [36] Zhou S, Yin T, Zou Q, Zhang K, Gao G, Shapter JG, *et al*. Labeling adipose derived stem cell sheet by ultrasmall super-paramagnetic Fe(3)O(4) nanoparticles and magnetic resonance tracking in vivo. *Sci Rep* 2017;7:42793. doi:10.1038/srep42793, PMID:28220818.
 - [37] Kleiner DE, Brunt EM, Van Natta M, Behling C, Contos MJ, Cummings OW, *et al*. Design and validation of a histological scoring system for nonalcoholic fatty liver disease. *Hepatology* 2005;41(6):1313–1321. doi:10.1002/hep.20701, PMID:15915461.
 - [38] Chen SD, Zhang H, Rios RS, Li YY, Zhu PW, Jin Y, *et al*. J-shaped relationship between serum zinc levels and the severity of hepatic necro-inflammation in patients with MAFLD. *Nutr Metab Cardiovasc Dis* 2022;32(5):1259–1265. doi:10.1016/j.numecd.2022.01.035, PMID:35260312.
 - [39] Ahmed U, Latham PS, Oates PS. Interactions between hepatic iron and lipid metabolism with possible relevance to steatohepatitis. *World J Gastroenterol* 2012;18(34):4651–4658. doi:10.3748/wjg.v18.i34.4651, PMID:23002334.
 - [40] Chen Z, Tian R, She Z, Cai J, Li H. Role of oxidative stress in the pathogenesis of nonalcoholic fatty liver disease. *Free Radic Biol Med* 2020;152:116–141. doi:10.1016/j.freeradbiomed.2020.02.025, PMID:32156524.
 - [41] Corradini E, Pietrangelo A. Iron and steatohepatitis. *J Gastroenterol Hepatol* 2012;27(Suppl 2):42–46. doi:10.1111/j.1440-1746.2011.07014.x, PMID:22320915.
 - [42] Zhou XD, Li YT, Kim SU, Yip TC, Petta S, Nakajima A, *et al*. Longitudinal Changes in Fibrosis Markers: Monitoring Stiffness/Fibrosis Progression and Prognostic Outcomes in MASLD. *Clin Gastroenterol Hepatol* 2025. doi:10.1016/j.cgh.2025.07.011, PMID:40714381.
 - [43] Handa P, Thomas S, Morgan-Stevenson V, Maliken BD, Gochanour E, Boukhar S, *et al*. Iron alters macrophage polarization status and leads to steatohepatitis and fibrogenesis. *J Leukoc Biol* 2019;105(5):1015–1026. doi:10.1002/JLB.3A0318-108R, PMID:30835899.
 - [44] Ganz T, Nemeth E. Iron homeostasis in host defence and inflammation. *Nat Rev Immunol* 2015;15(8):500–510. doi:10.1038/nri3863, PMID:26160612.
 - [45] Robson KJ, Lehmann DJ, Wilmhurst VL, Livesey KJ, Combrinck M, Merryweather-Clarke AT, *et al*. Synergy between the C2 allele of transferrin and the C282Y allele of the haemochromatosis gene (HFE) as risk factors for developing Alzheimer's disease. *J Med Genet* 2004;41(4):261–265. doi:10.1136/jmg.2003.015552, PMID:15060098.